THE JOURNAL OF PHYSICAL CHEMISTRY A

Article

pubs.acs.org/JPCA

One- and Two-Color Resonant Photoionization Spectroscopy of Chromium-Doped Helium Nanodroplets

Markus Koch,* Andreas Kautsch, Florian Lackner, and Wolfgang E. Ernst*

Institute of Experimental Physics, Graz University of Technology, Petersgasse 16, A-8010 Graz, Austria

ABSTRACT: We investigate the photoinduced relaxation dynamics of Cr atoms embedded into superfluid helium nanodroplets. One- and two-color resonant two-photon ionization (1CR2PI and 2CR2PI, respectively) are applied to study the two strong ground state transitions $z^7P^o_{2,3,4} \leftarrow a^7S_3$ and $y^7P^o_{2,3,4} \leftarrow a^7S_3$. Upon photoexcitation, Cr* atoms are ejected from the droplet in various excited states, as well as paired with helium atoms as Cr*–He_n exciplexes. For the $y^7P^o_{2,3,4}$ intermediate state, comparison of the two methods reveals that energetically lower states than previously identified are also populated. With 1CR2PI we find that the population of ejected $z^5P^o_3$ states is reduced for increasing droplet size, indicating that population is transferred preferentially to lower states during longer interaction with the droplet. In the 2CR2PI spectra we find evidence for generation of bare Cr atoms in their septet ground state (a^7S_3) and metastable quintet state (a^5S_2), which we attribute to a photoinduced fast excitation–relaxation cycle mediated by the droplet. A fraction of Cr atoms in these ground and metastable states is attached to helium atoms, as indicated by blue wings next to bare atom spectral lines. These relaxation channels provide new insight into the interaction of excited transition metal atoms with helium nanodroplets.

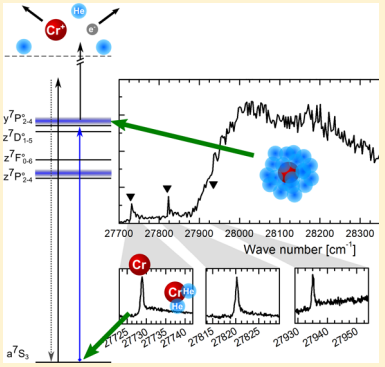

INTRODUCTION

The advent of helium nanodroplets (He_N) has spawned many new vistas in the field of matrix isolation spectroscopy.[1,2] Various fascinating spectroscopic experiments have been enabled by helium nanodroplet isolation spectroscopy, among them the study of the phenomenon of superfluidity from a microscopic perspective[3,4] or the investigation of high-spin molecules.[5−7] Helium droplets as well as bulk superfluid helium[8] offer a unique spectroscopic matrix because of the weak interaction with dopants. He_N with an internal temperature of 0.37 K can be easily combined with many spectroscopic techniques. Utilizing the method of resonant multiphoton ionization (REMPI) spectroscopy for the investigation of doped helium nanodroplets is well established and has recently enabled the study of unusual alkali metal–(He_N) Rydberg complexes[9−13] as well as tailored molecules and clusters.[14−16]

The investigation of complex magnetic phenomena in small nanoclusters is of interest for both fundamental theory of magnetism and the development of novel electronic devices. In this context, chromium (Cr) atoms with their huge magnetic moment[17] are of special interest. Cr nanoclusters exhibit a rich magnetic behavior and unusual properties, which are highly dependent on their geometric structure and spin configuration. A fundamental example of such an unusual and spin-dependent effect is the Kondo response of the triangular Cr trimer.[18] Helium nanodroplets are known to favor the formation of high-spin species,[6] which may offer a convenient way for the selective preparation of high-spin Cr nanoclusters and their subsequent surface deposition[19,20] under soft landing conditions.[21]

Recently, we started the investigation of Cr atoms and clusters embedded in He_N.[22−24] Mass spectroscopic studies demonstrated the formation of clusters consisting of up to 9 Cr atoms.[22] To gain deeper insight into the interaction between Cr atoms and the helium droplet, we focused on the spectroscopic study of single isolated Cr atoms in He_N. These experiments shine light on the influence of the droplet on the electronic structure of the Cr atom as well as photoinduced dynamics by utilizing various spectroscopic methods such as laser-induced fluorescence (LIF) spectroscopy, beam depletion (BD) spectroscopy and one-color resonant two-photon ionization (1CR2PI). Our previous studies cover the $y^7P^o_{2,3,4}$ and $z^5P^o_{1,2,3}$ states. The $y^7P^o_{2,3,4} \leftarrow a^7S_3$ transition appears broadened (600 cm^{-1}) and blue-shifted. In addition, transitions to discrete autoionizing (AI) states ($g^5D_{2,3,4}$ and $e^3D_{1,2,3}$), which are interacting with the ionization continuum,[23] were observed. Dispersed LIF spectra recorded upon excitation to $y^7P^o_{2,3,4}$ show narrow band bare atom emission from the $y^7P^o_2$, $z^5P^o_{1,2,3}$, and $z^7P^o_{2,3,4}$ states.[24] Both observations demonstrate that a fraction of the Cr atoms is ejected from the droplets upon photoexcitation to the $y^7P^o_{2,3,4}$ states. These experiments show that the dynamic processes induced by photoexcitation are governed by nonradiative, droplet-mediated relaxation mechanisms that result in the formation of bare Cr* atoms in various excited and metastable states.

Special Issue: A. W. Castleman, Jr. Festschrift

Received: February 5, 2014
Revised: April 4, 2014
Published: April 7, 2014

   dx.doi.org/10.1021/jp501285r | J. Phys. Chem. A 2014, 118, 8373–8379

In this article we extend our studies to previously uninvestigated spectral regimes. The utilization of two-color resonant two-photon ionization (2CR2PI) spectroscopy via the two strong ground state transitions ($z^7P^\circ_{2,3,4} \leftarrow a^7S_3$ and $y^7P^\circ_{2,3,4} \leftarrow a^7S_3$) offers new insights into the photoinduced dynamics of Cr−He_N and the interactions between Cr and He_N. 2CR2PI can be applied to energetically lower states due to the addition of a second laser with higher photon energy. In addition to the observation of bare atoms, we discuss the photoinduced generation of ground state Cr−He_n complexes and excited Cr*−He_n exciplexes. The formation of complexes consisting of excited atoms or molecules with several attached helium atoms is a general process initiated by the excitation of foreign species embedded in helium nanodroplets. These neutral "exciplexes" have been observed for example for surface bound atoms such as alkali metal[25−31] atoms and molecules and alkaline-earth metal atoms[32] as well as for species located inside the droplet.[33,34] Here we show that not only bare Cr atoms relax into the quintet or septet ground state but also the observed Cr−He_n complexes. Different ionization pathways that are competing with relaxation mechanisms are reflected in the difference between 1CR2PI and 2CR2PI spectra. The study of the droplet size dependence of a selected transition shows additional characteristics about the relaxation and ejection mechanisms.

EXPERIMENTAL SECTION

The experimental setup has been described in detail in previous publications.[23,24,35,36] In brief, the He_N beam is formed in a supersonic expansion of helium gas (purity 99.9999%) from a cooled nozzle (5 μm diameter, p_0 = 50 bar stagnation pressure, and T_0 = 10−24 K temperature). The droplet size is controlled by T_0 and follows a log−normal distribution with maximum values in the range $\hat{N} \approx 350$ (T_0 = 24 K) to $\hat{N} \approx 8300$ (T_0 = 13 K). The droplet beam is crossed at right angles along 10 mm of its path by an effusive Cr atom beam obtained from a home-built high temperature electron bombardment source arranged parallel below the droplet beam.[22] With this crossed beam geometry—and additional five small apertures to collimate the droplet beam—it can be ensured that no free atoms reach the detector. The heating power of the Cr source is optimized for single atom pick up (~1700 °C). The beam of Cr-doped He_N is crossed at right angles by laser beams inside the extraction region of a quadrupole mass spectrometer (QMS, Balzers QMG 422). This setup allows 1CR2PI and 2CR2PI mass spectroscopy where either the laser wavelength is scanned and the mass filter is set to the most abundant Cr isotope of 52 u (56 u for Cr−He) or the detected mass is scanned for a fixed laser wavelength. For 2CR2PI one laser is always kept at a constant wavelength of 308 nm (32 468 cm^{-1}).

For 1CR2PI the laser pulses are obtained from a dye laser (Lambda Physik FL3002, dyes: RDC 360 Neu for 27 600−28 800 cm^{-1}, Stilben 3 for 23 200−23 900 cm^{-1}, and Coumarin307 for 19 100−20 100 cm^{-1}) pumped by an excimer laser (Radiant Dyes RD-EXC-200, XeCl, 308 nm $\triangleq$ 32 468 cm^{-1}, ~20 ns pulse duration, 100 Hz repetition rate). For 2CR2PI a fraction of the 308 nm light is branched off and guided to the ionization region. The temporal overlap with the ~15 ns dye laser pulses is set to >10 ns. Both laser beams are moderately focused to a spot size of ~5 mm^2. For the two-color experiment both lasers are attenuated best possible to reduce the probability of dopant ionization by photons of a single wavelength. Reasonable pulse energies were found within 0.3−0.6 mJ for all four laser wavelength regimes (Stilben 3, RDC 360 Neu, Coumarin 307, and XeCl laser).

In principle, R2PI occurs via the absorption of two photons, which can be of the same or of different colors (1CR2PI and 2CR2PI, respectively). The tunable laser is scanned across a resonant state while the ion yield is recorded as a function of laser wavelength. For 2CR2PI a second laser with constant wavelength is present. Relaxation mechanisms after the first absorption step have to be taken into account. The energy level diagram of selected Cr atomic states[37] is shown in Figure 1

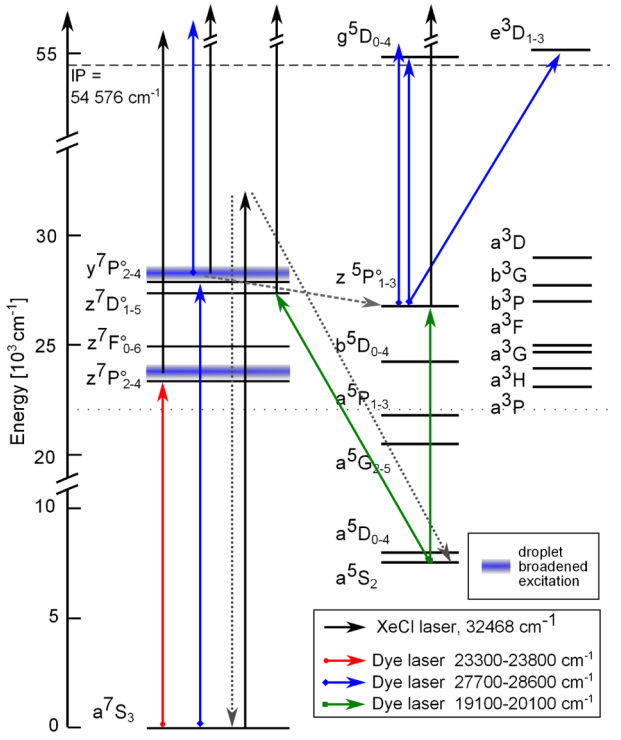

Figure 1. Energy level diagram for bare Cr atoms[37] showing 1CR2PI and 2CR2PI paths as combination of dye- and XeCl laser excitations and ionizations. The shaded areas above the $z^7P^\circ_{2,3,4}$ and $y^7P^\circ_{2,3,4}$ states indicate the droplet broadened and shifted excitation region. The dashed arrows indicate nonradiative relaxation paths. The dotted horizontal line at 22 108 cm^{-1} marks the lower limit above which ionization with a single XeCl laser photon (32 468 cm^{-1}) is possible.

together with various excitation and ionization paths for 1CR2PI and 2CR2PI. Due to the Cr ionization limit at 54575.6 ± 0.3 cm^{-1}[38] a successive absorption of at least two photons is required for ionization. The first step of the R2PI scheme is an excitation from the a^7S_3 ground state (electron configuration: $3d^54s$) to the excited states $z^7P^\circ_{2,3,4}$ ($3d^54p$) or $y^7P^\circ_{2,3,4}$ ($3d^44s4p$). The observed broadening and blue shift induced by the He_N are indicated as shaded areas above these levels. Both ground state excitations are accomplished by the tunable dye lasers in the regime of 23 200−23 900 cm^{-1} for $z^7P^\circ_{2,3,4}$ (red arrow in Figure 1) and 27 600−28 800 cm^{-1} for $y^7P^\circ_{2,3,4}$ (blue arrow). Upon excitation to $z^7P^\circ_{2,3,4}$ only a XeCl laser photon of 32 468 cm^{-1} (black arrow) has sufficient energy for ionization whereas for the $y^7P^\circ_{2,3,4}$ states photons of both the dye laser and the XeCl laser are able to ionize. The lower limit for PI with a single XeCl laser photon is marked by a dotted horizontal line. As indicated by the results, bare ground and metastable state Cr atoms and Cr−He_n complexes are produced in the course of 2CR2PI.

dx.doi.org/10.1021/jp501285r | J. Phys. Chem. A 2014, 118, 8373−8379

RESULTS AND DISCUSSION

$y^7P^\circ_{2,3,4} \leftarrow a^7S_3$ Excitation. We begin with the 2CR2PI excitation spectrum of the $y^7P^\circ_{2,3,4}$ ($3d^4 4s4p$) ← a^7S_3 ($3d^5 4s$) transition (bottom of Figure 2) because it can be compared

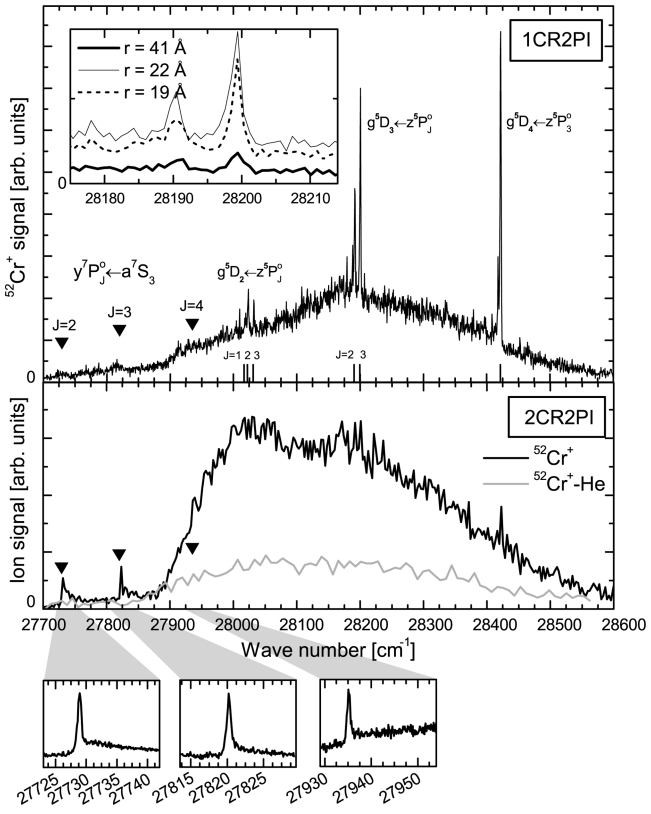

Figure 2. Top: 1CR2PI spectrum of the $y^7P^\circ_{2,3,4}$ ($3d^4 4s4p$) ← a^7S_3 ($3d^5 4s$) transition recorded by detecting $^{52}Cr^+$.[23] Bare atom ground state transitions are indicated by triangles.[37] The sharp lines can be assigned to transitions of bare, excited atoms to autoionizing states. The spectrum was recorded with T_0 = 20 K, and the inset shows scans in the $g^5D_3 \leftarrow z^5P^\circ_{2,3}$ region for other droplet sizes. Bottom: 2CR2PI spectrum of the same transition at comparable conditions, detected at the $^{52}Cr^+$ mass (52 u, black curve) and $^{52}Cr^+$–He mass (56 u, gray curve). Different scaling factors are used for the two spectra. Detailed scans in the region of bare atom transitions are also shown.

with the 1CR2PI spectrum of our previous work (top of Figure 2).[23] Cr^+ ions, which are detected at 52 u, are produced by in-droplet excitation with the tunable dye laser to the intermediate $y^7P^\circ_{2,3,4}$ states and subsequently ionized by a second photon either from the dye laser (1CR2PI) or from the XeCl laser (2CR2PI). In both $^{52}Cr^+$ spectra the width of the droplet broadened feature appears stretched over about 600 cm^{-1} to the blue side of the $y^7P^\circ_{2,3,4} \leftarrow a^7S_3$ bare atom transitions[37] (indicated by triangles in Figure 2). This is also in agreement with BD and LIF spectra.[24] As discussed in more detail in ref 23, this broadening depends on the change in electron configuration and is moderate compared to the same Cr transitions obtained in heavy rare-gas matrices[39] and comparable to the excitation spectra of other atomic species in He_N.[40] Although the onset of the broad structure occurs at the same wavelength in both cases, the 2CR2PI spectrum shows an additional shoulder in the range 27 900–28 100 cm^{-1} compared to the 1CR2PI spectrum. Upon in-droplet $y^7P^\circ_{2,3,4}$ excitation, ejection of bare Cr atoms in excited $z^5P^\circ_{1,2,3}$ states has previously been identified.[23,24] We take this increased signal in the 2CR2PI spectrum as indication for additional relaxation to states below $z^5P^\circ_{1,2,3}$. Because of the higher photon energy available in 2CR2PI (XeCl laser at 32 468 cm^{-1}) as compared to 1CR2PI, a number of excited states that may be populated (e.g., a^3P, z^7P°, a^3H, b^5D, a^3G, a^3F, z^7P°, cf., Figure 1) can add to the PI signal in the 2CR2PI scheme but not in 1CR2PI.

A 2CR2PI scan in the same spectral region with the mass filter tuned to the $^{52}Cr^+$–He mass (gray line in Figure 2, bottom) reveals a spectrum that is comparable in shape to the $^{52}Cr^+$ signal. This proves the formation of Cr*–He exciplexes during the relaxation–ejection process. The $^{52}Cr^+$–He signal is much weaker than that of $^{52}Cr^+$ (different scaling factors have been used for the two traces). However, no conclusions can be drawn about the Cr*/Cr*–He ratio because excess energy of the ionizing photon leads to fragmentation of the exciplexes at an unknown rate.

The appearance of sharper features also depends on the ionization scheme. In the 1CR2PI spectrum (Figure 2, top) sharp lines above 28 000 cm^{-1} represent the bare atom transitions from the excited $z^5P^\circ_{1,2,3}$ to the autoionizing states $g^5D_{2,3,4}$ and $e^3D_{1,2,3}$, as described in detail in ref 23. These transitions are barely visible in the 2CR2PI spectrum (Figure 2, bottom black curve). Upon ejection of excited Cr*, the presence of XeCl radiation in the 2CR2PI scheme provides a second ionization channel. This leads to a strong increase of PI into the continuum that apparently outweighs the transition to an AI state by a second resonant dye laser photon. Below 28 000 cm^{-1}, narrow structures are present at the bare atom $y^7P^\circ_{2,3,4} \leftarrow a^7S_3$ line positions in the 2CR2PI spectrum but not at all in the 1CR2PI spectrum. These asymmetric lines with a wing on the blue side are present in neither the BD nor LIF spectra.[24] We take these features as proof for the generation of bare, ground state (a^7S_3) Cr atoms and Cr–He_n molecules related to XeCl laser excitation of the 2CR2PI scheme (see discussion below). Due to our crossed pickup geometry we can exclude that bare atoms reach the ionization region directly. This is proven by two facts: first, without helium droplets but with a heated Cr source, we see absolutely no ion signal and, second, the 1CR2PI spectrum (Figure 2, top) has no sharp features at the bare atom line positions. Furthermore, we identify resonant excitations of Cr quintet metastable states (Figure 5), which cannot originate from the Cr source.

Droplet Size Dependence of Relaxation Mechanisms. The relaxation dynamics are influenced by the size of the droplets and we obtain information about this dependency from the 1CR2PI spectrum in the range of the $g^5D_3 \leftarrow z^5P^\circ_3$ AI transition (28 180–28 210 cm^{-1}, see inset of Figure 2). The AI peak height is proportional to the number of bare Cr atoms ejected from the droplet in the $z^5P^\circ_3$ state. The background signal, in contrast, corresponds to relaxation to other states that lie high enough in energy to be photoionized by the dye laser (e.g., y^7P°, b^3G, z^7D°, b^3P; note that all of these are higher in energy than $z^5P^\circ_3$). Also, Cr*–He_n exciplexes, even in case of a $z^5P^\circ_3$ Cr state, contribute to the background and not to the AI peak. Figure 3 shows the ratio of the AI peak height to the background. The peak height is obtained from a Gauss fit of the AI peak. Monitoring the ratio has the advantage that it is not influenced by variations of He_N flux with nozzle temperature. The AI peak height decreases almost by a factor of 3 with respect to the background for an increase of droplet radius from ~15 to ~46 Å. We take this as indication that for increasingly larger droplets relaxation to lower states than $z^5P^\circ_3$ occurs. In Ar

dx.doi.org/10.1021/jp501285r | J. Phys. Chem. A 2014, 118, 8373–8379

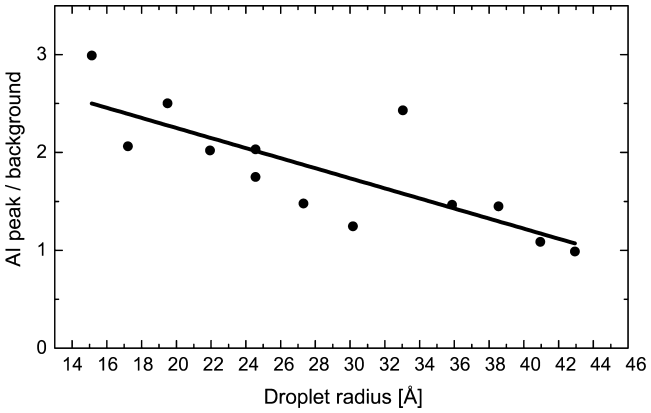

Figure 3. Ratio of atoms ionized through the g^5D_3 autoionization state ($g^5D_3 \leftarrow z^5P^\circ_3$ transition) to atoms ionized into continuum states in dependence on the droplet size. The line represents a linear fit and serves as guide to the eye.

matrices, where the perturbation by the host matrix is stronger and not limited in time because of ejection, Cr excitation to z^7P° leads primarily to relaxation to a^3P states, which are lower in energy than states we find to be populated.[39] Although species on the He_N surface also show relaxation,[25,32,41] our findings can be better compared to the Ag−He_N system, where excitation to the droplet broadened Ag $^2P_{3/2}$ structure leads to the ejection of bare Ag atoms in the $^2P_{1/2}$ state[33] and increasing the droplet size leads to an increase of Ag $^2P_{1/2}$ yield. The increased nonradiative transfer of population in excited Ag to the lowest excited state ($^2P_{1/2}$) for larger droplets supports our findings. In Cr the next lower state ($z^7F^\circ_6$) lies about 1000 cm^{-1} beneath $z^5P^\circ_3$ and, within a few thousand wavenumbers, a multitude of states with all multiplicities can be found.[37] Increased relaxation to lower states for longer interaction with the helium droplet during ejection from larger droplets seems thus to be reasonable.

$z^7P^\circ_{2,3,4} \leftarrow a^7S_3$ Excitation. The 2CR2PI spectrum via the $z^7P^\circ_{2,3,4}$ ($3d^54p$) as resonant intermediate state is shown in Figure 4 for the detection of $^{52}Cr^+$ (black) and $^{52}Cr^+$−He ions (gray). Upon comparison of the $^{52}Cr^+$ spectrum to beam depletion spectra,[24] it becomes evident that for both techniques the droplet broadened feature has the same onset at about 23 400 cm^{-1} and that it extends several hundred wavenumbers to the blue. For the 2CR2PI spectrum the spectral shape is given by the combination of in-droplet excitation, subsequent relaxation, ejection from the droplet and, finally, ionization. Only z^7P° and a^3P lie high enough in energy to be ionized by a XeCl laser photon (32 468 cm^{-1}); relaxation to lower states will not contribute to the ion signal. We thus expect that a major part of the excited atoms relax to lower states and do not contribute to the 2CR2PI spectrum. The $^{52}Cr^+$−He signal above 23 400 cm^{-1}, although very weak, demonstrates the formation of Cr*−He exciplexes upon excitation to $z^7P^\circ_{2,3,4}$, as for $y^7P^\circ_{2,3,4}$ excitation above (Figure 2).

Similar to the $y^7P^\circ_{2,3,4}$ intermediate state, narrow spectral structures appear in the $^{52}Cr^+$ detected spectrum at the bare atom $z^7P^\circ_{2,3,4} \leftarrow a^7S_3$ line positions, also showing a wing toward higher wavenumbers. As will be discussed below, this is an indication for the presence of bare a^7S_3 Cr atoms and Cr−He_n ground-state molecules.

Formation of Quintet State Atoms. To examine the population of other states than the septet ground state, PI spectra were recorded with the dye laser scanning over the

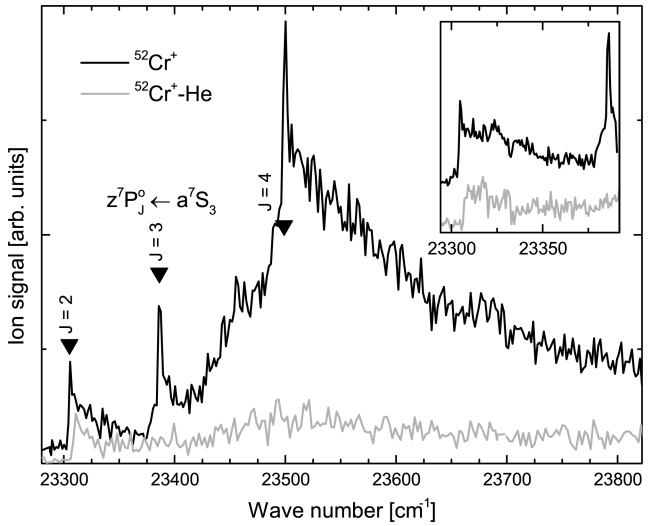

Figure 4. 2CR2PI excitation spectrum of the $z^7P^\circ_{2,3,4}$ ($3d^54p$) ← a^7S_3 ($3d^54s$) transition (T_0 = 20 K, $\hat{N}$ = 1300), recorded at the $^{52}Cr^+$ mass (52 u, black curve) and $^{52}Cr^+$−He mass (56 u, gray curve) with different scaling factors. The inset shows high resolution scans at both masses with vertical offsets. Bare atom $z^7P^\circ_{2,3,4} \leftarrow a^7S_3$ transitions[37] are indicated by triangles.

spectral regions of metastable quintet state transitions (green arrows in Figure 1) while the XeCl laser wavelength was fixed. As shown in Figure 5, we observe the population of the

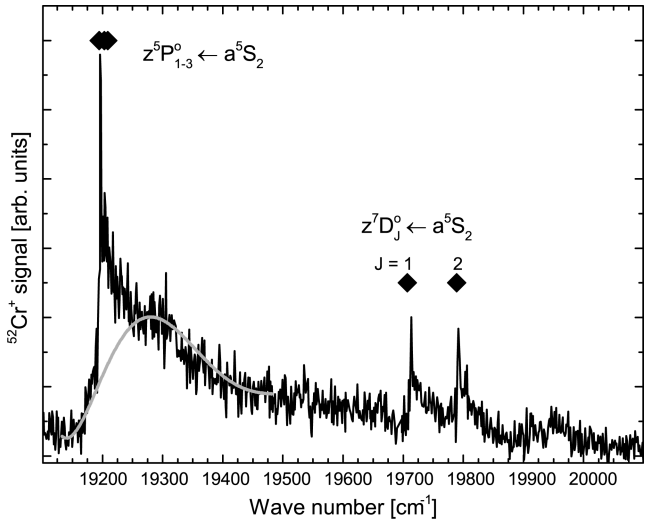

Figure 5. 2CR2PI excitation spectrum of the $z^5P^\circ_{1,2,3} \leftarrow a^5S_2$ and $z^7D^\circ_{1,2} \leftarrow a^5S_2$ transitions recorded at the $^{52}Cr^+$ mass (52 u). Bare atom transitions are indicated with squares.[37] The gray curve serves to indicate a broad structure of unknown origin.

metastable a^5S_2 ($3d^54s$) state. In yet another wavelength range we find evidence for population of another metastable quintet state by identifying the bare atom transitions originating from a^5D ($3d^44s^2$) (not shown). This can be taken as another proof that the atoms cannot origin directly from the evaporation source but have to experience a droplet-mediated relaxation. Clearly, the spectrum in Figure 5 is dominated by the strong free atom $z^5P^\circ_{1,2,3}$ ($3d^54p$) ← a^5S_2 ($3d^54s$) transition. The structure in the range 19 150−19 600 cm^{-1} is a superposition of a broad structure of unclear origin and sharp features at the bare atom $z^5P^\circ_{1,2,3} \leftarrow a^5S_2$ transitions. The broad structure is

dx.doi.org/10.1021/jp501285r | J. Phys. Chem. A 2014, 118, 8373−8379

schematically indicated with a gray line, starting to the red side of the free atom transitions and having a weak maximum at 19 300 cm^{-1}. The wing to the blue side of the $z^5P^\circ_{1,2,3} \leftarrow a^5S_2$ feature has thus a width of ~50 cm^{-1}. Within the observed energy region also the $z^7D^\circ_{1,2}$ $(3d^4 4s4p) \leftarrow a^5S_2$ $(3d^5 4s)$ intercombination lines appear as sharp free atom transitions with wings to the blue side. We note that although these are intercombination lines, they are listed in literature for bare atoms.[42]

Formation of Cr−He$_n$ Complexes and Cr*−He Exciplexes. Multiphoton ionization schemes of Cr−He$_N$ give rise to the detection of Cr^+−He$_n$ complexes in our current study. The abundance of Cr^+−He$_n$ with $n > 1$ is very low and the products are almost exclusively detected at the mass windows corresponding to Cr^+ atoms and Cr^+−He in the examined spectral regimes.

The formation of exciplexes, consisting of excited atoms or molecules with several attached helium atoms, has been observed upon photoexcitation for various species inside and on the surface of helium nanodroplets.[25−28,32−34] In these experiments it has been shown that REMPI spectroscopy allows to draw conclusions on the formation of intermediate neutral exciplexes only with some reservation because it probes the resultant ionic complexes. If the ionizing laser photon energy is higher than the vertical ionization potential, the generated ionic complex can carry internal energy, which may cause the evaporation of helium atoms from the ionic complexes. Consequently, our REMPI mass spectra do not necessarily reflect the abundance of exciplexes; moreover the number of He atoms attached to the dopant will be underestimated. In our experiments, the formation of Cr*−He exciplexes is observed. The Cr^+−He spectra presented in Figures 2 and 4 have a similar shape as the droplet broadened transitions monitored at the Cr^+ mass window. This shows that Cr*−He$_n$ exciplexes are formed and ejected upon photoexcitation with the dye laser. In contrast to other helium droplet isolation experiments, we find evidence for the presence of ground state Cr−He$_n$ complexes, which will be discussed in the following. These complexes are formed when the XeCl laser is present and are ionized by two-photon ionization; i.e., at least three photons are involved in the overall process that proceeds during the laser pulse duration (~20 ns).

A striking difference between the 2CR2PI and 1CR2PI spectra in Figure 2 is the emerging sharp spectral lines that correspond to the bare atom $y^7P^\circ_{2,3,4} \leftarrow a^7S_3$ transitions. The spectrally sharp transitions are accompanied by a small wing that extends toward the blue side. These spectral features are exclusively observed if the XeCl laser pulse is present. Similar transitions can be seen in the 2CR2PI spectra shown in Figures 4 and 5. Note that these features appear in addition to the droplet broadened structures and, especially, they are not present at the $y^7P^\circ_4 \leftarrow a^7S_3$ transition shown in the 1CR2PI spectrum (top Figure 2). In this region the dye laser excites a Cr−He$_N$ transition but does not give rise to a sharp spectral line. Furthermore, the sharp spectral lines shown in Figure 2 accompanied by blue wings are only present if the QMS is set to the Cr bare atom mass window.

Evidence for the connection of the blue wings to the formation of Cr−He$_n$ complexes can be seen in the inset of Figure 4 at the $z^7P^\circ_2$ $(3d^5 4p) \leftarrow a^7S_3$ $(3d^5 4s)$ transition. Therein the Cr^+ and Cr^+−He ion yields are compared (Cr^+ is vertically offset and the two signals are scaled with different factors). It can be seen that in contrast to the Cr^+ signal, the small wing but not the sharp lines are observed at the Cr^+−He mass (the low abundance of Cr^+−He_2 forbids the recording of an excitation spectrum for the corresponding mass window). Hence the origin of the sharp peaks can be attributed unambiguously to bare atoms in the a^7S_3 state. The fact that the wings are present in both mass windows and that they are only observed in the 2CR2PI spectra demonstrates that they must originate from Cr−He$_n$ ($n \geq 1$) products generated by a XeCl laser UV photon. It is important to note that in this spectral region, below the onset of the droplet broadened transition at 23 400 cm^{-1}, the signal corresponds exclusively to an excitation spectrum of products formed by the XeCl laser. Above 23 400 cm^{-1} the production of ground state Cr and Cr−He$_n$ by the XeCl laser is competing with dye laser excitation of Cr−He$_N$. We think that the absence of pronounced wings in the Cr^+−He signal for the $z^7P^\circ_{3,4}$ $(3d^5 4p) \leftarrow a^7S_3$ $(3d^5 4s)$ transitions in Figure 4 is related to the competition between these two excitation paths. Alternatively, the ability of excited Cr atoms to bind He atoms might be higher for the $z^7P^\circ_2$ state than for the $z^7P^\circ_{3,4}$ states. At the $y^7P^\circ_{2,3,4}$ $(3d^4 4s4p) \leftarrow a^7S_3$ $(3d^5 4s)$ transitions in Figure 2 the signal-to-noise ratio in the Cr^+−He signal was unfortunately too low, which forbids a comparison to the Cr^+ signal near the small blue wings.

The observation of these wings is remarkable because these Cr−He$_n$ complexes must be in their electronic septet or quintet ground state. Recent calculations of our group[43] show that the lowest Cr−He quintet and septet states are very weakly bound (a few wavenumbers, only one vibrational level is supported) with large internuclear separation (R_e > 5 Å). Calculations for coinage metals show that the binding energy rises with increasing number of helium atoms attached to the metal atom.[44] For the ground state, the coinage metals with their completely filled d-orbitals and one electron in the s-orbital, and chromium with its half-filled d-orbitals and one s-electron are very similar in their interaction with He atoms, which is dictated mainly by the electron in the s-orbital.[43] Consequently, the observed spectrum suggests that larger Cr−He$_n$ complexes are formed upon UV excitation, followed by droplet-mediated relaxation via various routes into the electronic septet and quintet (and probably also into the triplet) ground states. Note that this process must be completed in less than 20 ns, the pulse duration of the synchronized excitation and ionization lasers. The observed narrow structures represent the spectral signature of a transition that originates from a very weakly bound ground state at large internuclear distances into the slightly repulsive part of an intermediate Cr−He$_n$ state. This is expected from the Cr−He diatomic potential energy curves in ref 43. The excess energy of the laser and the internal energy of the formed Cr^+−He$_n$ complex will cause fragmentation of the intermediate complexes, which explains the observation of mainly Cr^+ and Cr^+−He in the mass spectrum. Consequently, REMPI spectroscopy forbids conclusions on the size of the intermediate Cr−He$_n$ complexes. From the present data we cannot exclude a surface migration of Cr atoms upon UV excitation. A similar scenario has been suggested for excited NO* molecules on helium nanodroplets.[34] The investigated Cr transitions can be compared to the 4p ← 4s transition in potassium, which is located on the droplet surface.[45] Similar to Cr−He$_n$, the potassium transition exhibits a characteristic narrow, asymmetric shape as well as a coincidence of the bare atom transition with the rising edge of the droplet broadened transition. More sophisticated calculations will assist the

dx.doi.org/10.1021/jp501285r | J. Phys. Chem. A 2014, 118, 8373−8379

assignment of the transitions to a small or large Cr−He$_n$ parent complex.

On the basis of our data we cannot draw conclusions on the process that underlies the formation of ground state and metastable Cr atoms and Cr−He$_n$ complexes because the spectral regime above the y^7P° state is not covered by our dye laser. We propose two different scenarios for the production of ground state and metastable Cr atoms and Cr−He$_n$. (i) Septet states are absent in the concerning spectral regime, but states with other multiplicities lie in the vicinity of the XeCl laser photon energy. Transitions from the septet ground state into states with other multiplicities, as they are observed for Cr (Figure 5), may be excited and responsible for the production of ground state and metastable state complexes. (ii) At our experimental conditions, Cr dimers are present in a certain fraction of helium droplets. The excitation of a dimer transition in the concerning spectral region may give rise to the production of various products such as Cr + Cr*−He$_n$, Cr* + Cr−He$_n$, or Cr*$_2$. The formation of Cr dimers is observed in helium nanodroplets,[22] and their spectra will be explored in the near future.

SUMMARY AND CONCLUSION

Chromium atoms doped to superfluid helium nanodroplets are investigated with one- and two-color resonant two-photon ionization spectroscopy (1CR2PI and 2CR2PI, respectively) via the $y^7P^\circ_{2,3,4}$ resonant intermediate states and with 2CR2PI via the $z^7P^\circ_{2,3,4}$ states. We find two independent indications that nonradiative population transfer of excited Cr* atoms mediated by the droplet takes place to lower states than previously identified.[23,24] For the $y^7P^\circ_{2,3,4}$ intermediate states, comparison of 1CR2PI and 2CR2PI is possible and an additional shoulder observed with 2CR2PI indicates the population of Cr* states that are too low in energy to be detected with 1CR2PI. Additionally, a decrease of $z^5P^\circ_3$ population of bare Cr* atoms for increasing droplet size also points toward relaxation to energetically lower states as the duration of interaction with helium during ejection is increased. The formation of Cr*−He$_n$ exciplexes upon in-droplet excitation of y^7P° and z^7P° is demonstrated by the fact that the excitation spectra obtained with Cr^+ and Cr^+−He detection are identical.

All 2CR2PI spectra reveal sharp lines at the bare atom positions, which we attribute to the presence of the 308 nm XeCl laser. A fast (<20 ns) excitation−relaxation cycle produces bare Cr atoms in the septet ground state (a^7S_3) as well as metastable quintet (a^5S_2 and a^5D) states, which are subsequently probed by 2CR2PI. All of these lines show a wing on their blue side, which indicates the presence of ground and metastable Cr−He$_n$ molecules. In addition, the detection of Cr^+−He ions in spectral regions of the $z^7P^\circ_2 \leftarrow a^7S_3$ wing verifies the presence of ground state Cr−He$_n$ complexes. Given the weak binding energy of ground-state septet and quintet Cr−He diatomic molecules[43] and the presumably only slightly stronger bond of Cr−He$_n$ complexes,[44] this observation is remarkable as it demonstrates that a complete relaxation to the Cr ground state has to take place inside the droplet.

The complex electronic structure of the Cr atom leads to even more complex electronic structure inside a helium droplet due to the perturbation by the surrounding helium. Several different relaxation channels to repulsive states that cause an ejection from the droplet might compete. The fact that Cr ions with attached helium atoms are detected in our experiments suggests that Cr−He$_n$ formation needs to be considered for the explanation of relaxation pathways and the description of the dynamics of Cr atoms inside helium droplets, calling for more sophisticated theoretical models. The Cr−He potential energy curves calculated in our group[43] can serve as a starting point for this task. Finally, it cannot be decided from our current data if ground state Cr atoms and Cr−He$_n$ complexes originate from excitation of single Cr atoms inside He_N or a photoinduced dissociation of Cr dimers inside the droplet. Photoexcitation of Cr dimers is subject of our current research.

AUTHOR INFORMATION

Corresponding Authors

*M. Koch: e-mail, markus.koch@tugraz.at.

*W. E. Ernst: e-mail, wolfgang.ernst@tugraz.at.

Notes

The authors declare no competing financial interest.

ACKNOWLEDGMENTS

We thank Matthias Hasewend and Friedrich Lindebner for experimental support as well as Johann V. Pototschnig and Martin Ratschek for helpful discussions. This work was supported by the Austrian Science Fund (FWF, Grant 22962-N20), as well as the European Commission and the Styrian Government within the ERDF program.

REFERENCES

(1) Callegari, C.; Ernst, W. E. In *Helium Droplets as Nanocryostats for Molecular Spectroscopy - from the Vacuum Ultraviolet to the Microwave Regime. - in: Handbook of High-Resolution Spectroscopy*; Merkt, F., Quack, M., Eds.; John Wiley & Sons: Chinchester, 2011.

(2) Toennies, J. P.; Vilesov, A. F. Spectroscopy of Atoms and Molecules in Liquid Helium. *Annu. Rev. Phys. Chem.* **1998**, *49*, 1−41.

(3) Grebenev, S.; Toennies, J. P.; Vilesov, A. F. Superuidity Within a Small Helium-4 Cluster: The Microscopic Andronikashvili Experiment. *Science* **1998**, *279*, 2083−2086.

(4) Tang, J.; Xu, Y.; McKellar, A. R. W.; Jäger, W. Quantum Solvation of Carbonyl Suldewith Helium Atoms. *Science* **2002**, *297*, 2030−2033.

(5) Higgins, J.; Callegari, C.; Reho, J.; Stienkemeier, F.; Ernst, W. E.; Lehmann, K. K.; Gutowski, M.; Scoles, G. Photoinduced Chemical Dynamics of High-Spin Alkali Trimers. *Science* **1996**, *273*, 629−631.

(6) Higgins, J.; Ernst, W. E.; Callegari, C.; Reho, J.; Lehmann, K. K.; Scoles, G.; Gutowski, M. Spin Polarized Alkali Clusters: Observation of Quartet States of the Sodium Trimer. *Phys. Rev. Lett.* **1996**, *77*, 4532−4535.

(7) Hauser, A. W.; Auböck, G.; Ernst, W. E. In *Jahn-Teller Effect and Spin-Orbit Coupling in Heavy Alkali Trimers - in: Vibronic Interactions and the Jahn-Teller Effect: Theory and Applications*; Atanasov, M., Daul, C., Tregenna-Piggott, P., Eds.; Springer Series: Progress in Theoretical Chemistry and Physics; Springer: 2012; Vol. *23*; Chapter 16, pp 301 − 316.

(8) Moroshkin, P.; Hofer, A.; Weis, A. Atomic and Molecular Defects in Solid ^{4}He. *Phys. Rep.* **2008**, *469*, 1−57.

(9) Lackner, F.; Krois, G.; Koch, M.; Ernst, W. E. Rubidium on Helium Droplets: Analysis of an Exotic Rydberg Complex for $n^* < 20$ and $0 \leq l \leq 3$. *J. Phys. Chem. Lett.* **2012**, *3*, 1404−1408.

(10) Lackner, F.; Krois, G.; Theisen, M.; Koch, M.; Ernst, W. E. Spectroscopy of nS, nP,and nD Rydberg Series of Cs Atoms on Helium Nanodroplets. *Phys. Chem. Chem. Phys.* **2011**, *13*, 18781−18781.

(11) Lackner, F.; Krois, G.; Ernst, W. E. Rydberg-Ritz Analysis and Quantum Defects for Rb and Cs Atoms on Helium Nanodroplets. *Mol. Phys.* **2013**, *111*, 2118−2125.

(12) Loginov, E.; Drabbels, M. Unusual Rydberg System Consisting of a Positively Charged Helium Nanodroplet with an Orbiting Electron. *Phys. Rev. Lett.* **2011**, *106*, 083401−1−083401−4.

(13) Loginov, E.; Callegari, C.; Ancilotto, F.; Drabbels, M. Spectroscopy on Rydberg States of Sodium Atoms on the Surface of Helium Nanodroplets. *J. Phys. Chem. A* **2011**, *115*, 6779−6788.
(14) Nagl, J.; Auböck, G.; Hauser, A. W.; Allard, O.; Callegari, C.; Ernst, W. E. Heteronuclear and Homonuclear High-Spin Alkali Trimers on Helium Nanodroplets. *Phys. Rev. Lett.* **2008**, *100*, 063001−1−063001−4.
(15) Mudrich, M.; Bünermann, O.; Stienkemeier, F.; Dulieu, O.; Weidemüller, M. Formation of Cold Bialkali Dimers on Helium Nanodroplets. *Eur. Phys. J. D* **2004**, *31*, 291−299.
(16) Krois, G.; Pototschnig, J. V.; Lackner, F.; Ernst, W. E. Spectroscopy of Cold LiCa Molecules Formed on Helium Nanodroplets. *J. Phys. Chem. A* **2013**, *117*, 13719−13731.
(17) Roos, B.; Borin, A.; Gagliardi, L. Reaching the Maximum Multiplicity of the Covalent Chemical Bond. *Angew. Chem., Int. Ed.* **2007**, *46*, 1469−1472.
(18) Jamneala, T.; Madhavan, V.; Crommie, M. Kondo Response of a Single Antiferromagnetic Chromium Trimer. *Phys. Rev. Lett.* **2001**, *87*, 256804−1−256804−4.
(19) Volk, A.; Thaler, P.; Koch, M.; Fisslthaler, E.; Grogger, W.; Ernst, W. E. High Resolution Electron Microscopy of Ag-Clusters in Crystalline and Non-crystalline Morphologies Grown Inside Superuid Helium Nanodroplets. *J. Chem. Phys.* **2013**, *138*, 214312−1−214312−7.
(20) Gomez, L. F.; Loginov, E.; Vilesov, A. F. Traces of Vortices in Superuid Helium Droplets. *Phys. Rev. Lett.* **2012**, *108*, 155302−1−155302−5.
(21) Thaler, P.; Volk, A.; Ratschek, M.; Koch, M.; Ernst, W. E. Molecular Dynamics Simulation of the Deposition Process of Cold Ag-Clusters under Different Landing Conditions. *J. Chem. Phys.* **2014**, *140*, 044326−1−044326−9.
(22) Ratschek, M.; Koch, M.; Ernst, W. E. Doping Helium Nanodroplets with High Temperature Metals: Formation of Chromium Clusters. *J. Chem. Phys.* **2012**, *136*, 104201−1−104201−6.
(23) Kautsch, A.; Hasewend, M.; Koch, M.; Ernst, W. E. Fano Resonances in Chromium Photoionization Spectra after Photoinduced Ejection from a Superuid Helium Nanodroplet. *Phys. Rev. A: At. Mol. Opt. Phys.* **2012**, *86*, 033428−1−033428−4.
(24) Kautsch, A.; Koch, M.; Ernst, W. E. Electronic Relaxation after Resonant Laser Excitation of Cr in Superuid Helium Nanodroplets. *J. Phys. Chem. A* **2013**, *117*, 9621−9625.
(25) Brühl, F. R.; Trasca, R. A.; Ernst, W. E. Rb-He Exciplex Formation on Helium Nanodroplets. *J. Chem. Phys.* **2001**, *115*, 10220−10224.
(26) Reho, J.; Callegari, C.; Higgins, J.; Ernst, W. E.; Lehmann, K. K.; Scoles, G. Spin-orbit Effects in the Formation of the Na-He Excimer on the Surface of He Clusters. *Faraday Discuss.* **1997**, *108*, 161−174.
(27) Theisen, M.; Lackner, F.; Ernst, W. E. Cs Atoms on Helium Nanodroplets and the Immersion of Cs^+ into the Nanodroplet. *J. Chem. Phys.* **2011**, *135*, 074306−1−074306−7.
(28) Theisen, M.; Lackner, F.; Ernst, W. E. Forming Rb^+ Snowballs in the Center of He Nanodroplets. *Phys. Chem. Chem. Phys.* **2010**, *12*, 14861−14863.
(29) Schulz, C. P.; Claas, P.; Stienkemeier, F. Formation of K*He Exciplexes on the Surface of Helium Nanodroplets Studied in Real Time. *Phys. Rev. Lett.* **2001**, *87*, 153401−1−153401−4.
(30) Droppelmann, G.; Bünermann, O.; Schulz, C. P.; Stienkemeier, F. Formation Times of RbHe Exciplexes on the Surface of Superuid versus Normal Fluid Helium Nanodroplets. *Phys. Rev. Lett.* **2004**, *93*, 023402−1−023402−4.
(31) Giese, C.; Mullins, T.; Grüner, B.; Weidemüller, M.; Stienkemeier, F.; Mudrich, M.; Stienkemeier, F.; Mudrich, M. Formation and Relaxation of RbHe Exciplexes on He Nanodroplets Studied by Femtosecond Pump and Picosecond Probe Spectroscopy. *J. Chem. Phys.* **2012**, *137*, 244307−1−244307−7.
(32) Loginov, E.; Drabbels, M. Spectroscopy and Dynamics of Barium-Doped Helium Nanodroplets. *J. Chem. Phys.* **2012**, *136*, 154302−1−154302−12.
(33) Loginov, E.; Drabbels, M. Excited State Dynamics of Ag Atoms in Helium Nanodroplets. *J. Phys. Chem. A* **2007**, *111*, 7504−7515.
(34) Polyakova, E.; Stolyarov, D.; Wittig, C. Multiple Photon Excitation and Ionization of NO in and on Helium Droplets. *J. Chem. Phys.* **2006**, *124*, 214308−1−214308−11.
(35) Lindebner, F.; Kautsch, A.; Koch, M.; Ernst, W. E. Laser Ionization and Spectroscopy of Cu in Superuid Helium Nanodroplets. *Int. J. Mass Spectrom.* **2014**, DOI: 10.1016/j.ijms.2013.12.022.
(36) Koch, M.; Lanzersdorfer, J.; Callegari, C.; Muenter, J. S.; Ernst, W. E. Molecular Beam Magnetic Resonance in Doped Helium Nanodroplets. A Setup for Optically Detected ESR/NMR in the Presence of Unresolved Zeeman Splittings. *J. Phys. Chem. A* **2009**, *113*, 13347−13356.
(37) Sugar, J.; Corliss, C. Atomic-Energy Levels of The Iron-Period Elements - Potassium Through Nickel. *J. Phys. Chem. Ref. Data* **1985**, *14*.
(38) Huber, M. C. E.; Sandeman, R. J.; Tubbs, E. F. The Spectrum of Cr I between 179.8 and 200 nm Wavelengths, Absorption Cross Sections, and Oscillator Strengths. *Proc. R. Soc. London, Ser. A* **1975**, *342*, 431−438.
(39) Pellin, M. J.; Gruen, D. M.; Fisher, T.; Foosnaes, T. Emission, Optical-optical Double Resonance, and Excited State Absorption Spectroscopy of Matrix Isolated Chromium and Molybdenum Atoms. *J. Chem. Phys.* **1983**, *79*, 5871−5886.
(40) Bartelt, A.; Close, J. D.; Federmann, F.; Quaas, N.; Toennies, J. P. Cold Metal Clusters: Helium Droplets as a Nanoscale Cryostat. *Phys. Rev. Lett.* **1996**, *77*, 3525−3528.
(41) Fechner, L.; Gruner, B.; Sieg, A.; Callegari, C.; Ancilotto, F.; Stienkemeier, F.; Mudrich, M. Photoionization and Imaging Spectroscopy of Rubidium Atoms Attached to Helium Nanodroplets. *Phys. Chem. Chem. Phys.* **2012**, *14*, 3843−3851.
(42) Kramida, A.; Yu. Ralchenko, Reader, J. and NIST ASD Team (2012). NIST Atomic Spectra Database (ver. 5.0), [Online]. Available: http://physics.nist.gov/asd [2013, May 16]. National Institute of Standards and Technology: Gaithersburg, MD.
(43) Pototschnig, J. V.; Ratschek, M.; Hauser, A. W.; Ernst, W. E. An Ab Initio Study of the CrHe Diatomic Molecule: The Effect of Van Der Waals Distortion on a Highly Magnetic Multi-electron System. *Phys. Chem. Chem. Phys.* **2014**, DOI: 10.1039/C4CP00559G.
(44) Cargnoni, F.; Mella, M. Solubility of Metal Atoms in Helium Droplets: Exploring the Effect of the Well Depth Using the Coinage Metals Cu and Ag. *J. Phys. Chem. A* **2011**, *115*, 7141−7152.
(45) Stienkemeier, F.; Higgins, J.; Callegari, C.; Kanorsky, S.; Ernst, W. Spectroscopy of Alkali Atoms (Li, Na, K) Attached to Large Helium Clusters. *Z. Phys. D: Atom. Mol. Cl.* **1996**, *38*, 253−263.